Description and application of an analytical model to quantify downward smoke displacement caused by a water spray

Zhi Tang[1,2], Jan Vierendeels[2], Zheng Fang[1] and Bart Merci[2]
[1]Wuhan University - School of Civil Engineering, Wuhan, China
[2]Ghent University - Dept. of Flow, Heat and Combustion Mechanics, Ghent, Belgium

Abstract

An analytical model is developed from basic principles to quantify the downward smoke displacement as caused by a water spray from e.g. a sprinkler head. The underlying assumptions are identified and the global balance is described between downward drag force, potentially downward buoyancy due to a cooling effect within the water spray envelope in the smoke layer, and the upward buoyant force in the ambient air below the smoke layer. From this balance, the downward smoke displacement is quantified. It is explained that the classical Bullen theory to define a criterion for smoke layer stability is in general not valid. There is always downward smoke displacement, although potentially small, depending on the circumstances. The tracking of individual water droplets leads to the evolution of the spray envelope radius and provides the total downward drag force on the smoke. An extensive sensitivity study is presented, varying the water spray angle at the nozzle, the water droplet diameter, the smoke layer temperature, and inclusion or not of the cooling effect by water and air entrainment in the downward smoke displacement. It is highlighted that the downward smoke displacement is more pronounced for smaller droplets (for fixed water mass flow rate), and for lower smoke layer temperatures. For larger water spray angle at the nozzle, the downward displacement also increases monotonically with initial smoke layer thickness. A smaller spray angle at the nozzle leads to stronger

downward smoke displacement and the variation of downward smoke displacement with initial smoke layer thickness is non-monotonic: stronger descent of smoke for thinner smoke layer, but beyond a critical smoke layer thickness also again a stronger descent with increasing smoke layer thickness. The accuracy of the model as presented is illustrated by means of an experimental data set.

Keywords: Fire smoke; Water spray; Sprinkler; Water droplet

Nomenclature

C_D	drag coefficient
C_d	discharge coefficient of the nozzle
d_c	distance from ceiling to nozzle (m)
d_m	volume median diameter of water droplets (μ m)
d_n	orifice diameter of nozzle (mm)
F_B	buoyancy force (N)
F_d	drag force on single water droplet (N)
F_{d_r}	drag force on single water droplet in r-direction (N)
F_{d_z}	drag force on single water droplet in z-direction (N)
F_D	total drag force (N)
g	gravity acceleration ($m \cdot s^{-2}$)
h	distance from nozzle to the bottom of the smoke layer before discharging water droplets (m)
Δh	downward smoke displacement (m)
m	single water droplet mass (kg)
m_w	total water droplets mass in Zone II (kg)
$\dot{m}_w$	water mass flow rate (kg/s)
P	operating pressure of the sprinkler (MPa)
Re	Reynolds number
t	time of the water droplet travelling through the smoke layer (s)
T_a	ambient air temperature (K)
T_{aih}	average temperature of the smoke inside the hood (K)
$T_{i,a}$	smoke temperature in sprinkler spray region surrounded by ambient air (K)
$T_{i,s}$	smoke temperature in sprinkler spray region surrounded by smoke (K)
T_s	smoke temperature outside sprinkler spray region (K)

v_r	radial velocity of the water droplet (m/s)
v_z	vertical velocity of the water droplet (m/s)
v	velocity of the water droplet (m/s)
v_{in}	initial velocity of the water droplet (m/s)
$v_{r,in}$	initial radial velocity of the water droplet (m/s)
$v_{z,in}$	initial vertical velocity of the water droplet (m/s)
$v_{z,out}$	final vertical velocity of the water droplet (m/s)
$V_{i,s}$	The volume of the sprinkler spray region surrounded by smoke (m^3)
$V_{i,a}$	The volume of the sprinkler spray region surrounded by ambient air (m^3)
ρ_a	ambient air density (kg/m^3)
ρ_d	water density (kg/m^3)
$\rho_{i,s}$	smoke density inside the sprinkler spray region surrounded by smoke (kg/m^3)
$\rho_{i,a}$	smoke density inside the sprinkler spray region surrounded by ambient air (kg/m^3)
ρ_s	smoke density outside the sprinkler spray region (kg/m^3)
θ	water spray angle ($\circ$)

1. Introduction

The automatic sprinkler/water mist spray system has been widely adopted as possible fire protection facility in buildings due to its good performance in extinguishing fire or controlling the fire scale (size and heat release rate (HRR)). However, such a system can cool down the smoke layer and the water droplets exert a downward drag force onto the smoke. Both effects lead to “smoke logging”, a downward displacement of the smoke layer affected by water droplets [2-4].

Generally, during the early stages of an enclosure fire, due to buoyancy the fire smoke forms a stratified hot smoke layer beneath ceiling and keeps a relatively clean environment in lower regions, where there can be a route for occupants to evacuate from the building. When discharging water droplets, smoke logging is observed in real fires and experimental studies [2-5]. The downward displacement of smoke layer can pose a great risk for occupants, since the effect of reduced visibility delays escape and increases the duration of exposure of the occupants of a building to the products of combustion. Consequently, it is important to understand the downward displacement of fire smoke under water spray conditions.

In the literature, many studies are found on the topic of interaction of water droplets with fire smoke layer [1-18]. The cooling effect and drag force produced by water droplets are considered generally to yield smoke logging [1-8]. Bullen [2] presented a theory, leading to an instability criterion of smoke layer under water spray conditions. The criterion is based on the ratio of drag force of water droplets (D) to buoyancy of smoke layer (B). The schematic figure is shown in Figure 1.

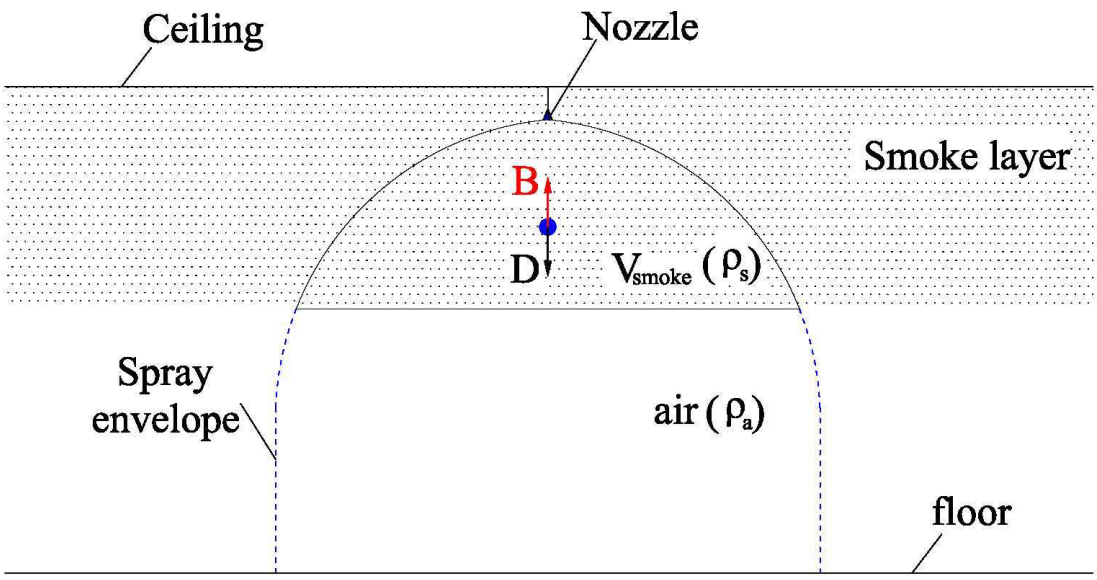

Figure1 Schematic of instability criterion from Bullen theory

Smoke logging would happen when D > B; otherwise, the layer remains stable. This theory is adopted also in recent publications, e.g. [3-4, 6]. However, we explain in the present paper how this theory must be revised, starting from first principles. Indeed, several sets of independent experiments [3, 12-13] show a loss of stability of the smoke layer that cannot be explained by Bullen's criterion. Zhang [12] and Li [3] established their own criteria, starting from Bullen's theory, by considering the smoke layer temperature gradient and the spatial distribution of the drag force in the spray region respectively. Comparisons between these three criteria with experiments [2, 12-13] indicate smoke logging can happen when D < B in some cases.

Actually, the issue is more fundamental. Eq. (1) is usually adopted to calculate the smoke layer buoyancy (B) in two-layer zone models [2 - 4, 18].

$$B = (\rho_a - \rho_s) g V_{smoke} \tag{1}$$

where ρ_a is the air density, ρ_s is the smoke density and V_{smoke} is the volume of smoke in spray envelope, as shown in Figure 1.

According to Archimedes Law, Eq. (1) is suitable only if V_{smoke} is entirely surrounded by air at ambient temperature. In reality, however, this is never the case. On the contrary, the buoyancy force works downward on smoke that is cooled by the water from the sprinklers / water mist, since it is surrounded by hot smoke. Only the lower part of V_{smoke} is surrounded by ambient air and therefore upward buoyancy can only apply to that region. As such, using Eq. (1) to calculate the buoyancy force (B) for Bullen's criterion is in general not correct. Only as long as the initial smoke layer is not too thick (and thus most of the spray envelope is in fact surrounded by ambient air), Eq. (1) is a reasonable approximation of reality.

Therefore, the aim of the present work is to provide a more correct and more generally applicable analytical model to quantitatively depict smoke logging due to sprinkler / water mist water. The model is tested by comparison to experimental data [3]. Afterwards, the main influence factors for smoke logging are revealed by performing a sensitivity study with the developed model.

2. Model development

The model focuses on the interaction between water droplets and a steady smoke layer. The location is therefore supposed to be far away from the fire source. On the one hand, interaction with the fire or with upward flowing smoke is as such avoided. Furthermore, smoke logging is also more likely in cooler smoke and potentially more harmful for occupants. At the moment, a possible horizontal velocity in the smoke layer is not included (although it is not difficult to extend the model to this purpose, as discussed below). The schematic figure is shown in Figure 2.

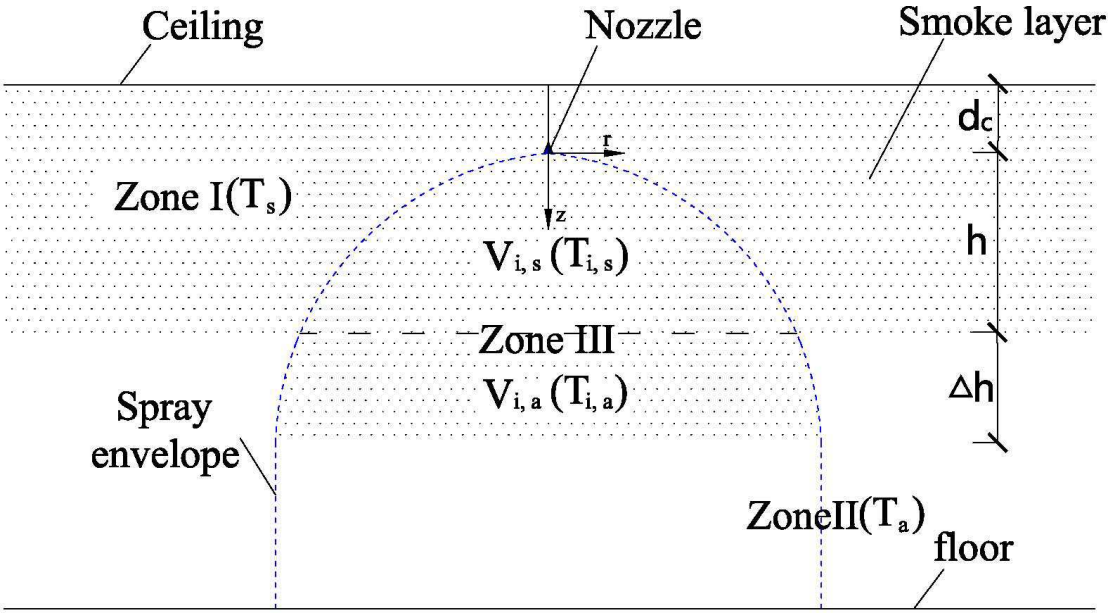

Figure 2 Schematic sketch of model ingredients.

2.1 Mechanisms for smoke logging

Smoking logging results from the combined effect of:

- Cooling effect: a certain volume of the smoke can be cooled down by the water droplets;
- Drag force: the water droplets exert a downward drag force onto the smoke.

Water droplets cool down the hot smoke in a spray envelope (Zone III in Figure 2) by convective heat transfer, radiative heat absorption and evaporative heat absorption [10]. The rate of vaporisation of a droplet depends upon its surface area, the heat transfer

coefficient and the relative velocity between the droplet and the surrounding gas [20-21]. As a result, the smoke layer inside the spray envelope is surrounded by smoke with higher temperature. This means that the density of the smoke layer inside the spray envelope is higher than that of the surrounding smoke layer, resulting in a net 'downward buoyancy force' within the smoke layer, one possible reason for smoke logging.

The other reason for smoke logging is the drag force acting on the smoke as the water droplets travel through the smoke layer. The total drag force depends on the number of water droplets, drag coefficient (C_D), and the velocity of the droplets, relative to the smoke. For the case at hand in the present paper, the drag force is more important than the net downward buoyancy force (see below).

2.2 Model assumptions

Three zones are distinguished in the model, based on temperature differences (Figure 2):

- Zone I: the smoke layer outside the water spray envelope. This zone has the highest average temperature: the smoke is not affected by water droplets. The temperature (T_s) is supposed to be 'unaffected' by the water and is equal to the average smoke temperature without activation of the sprinkler/water mist system.
- Zone II: there is no smoke in Zone II, and the average temperature remains equal to ambient air temperature (T_a).
- Zone III: This zone is occupied by smoke inside the spray envelope. Zone III is divided into an upper part in the smoke region (Volume: $V_{i,s}$; Temperature: $T_{i,s}$) and a lower part in the ambient air region (Volume: $V_{i,a}$; Temperature: $T_{i,a}$). The temperature in the lower part can be lower than the temperature in the upper part due to entrainment of ambient air into the smoke logging region (see below).

Obviously, Fig. 2 is a simplified representation of the more complex reality. Yet, it allows the development of the analytical model as described below.

Interactions between water droplets and the smoke layer are very complex, e.g. due to turbulence and non-linear variation of physical properties [18]. However, we do not pursue complex simulations of individual detailed interactions among droplets. Rather, we target a global analytical model that allows interpretation of trends observed in smoke logging. Therefore, the following assumptions are made here to simplify the model:

- The smoke layer is quiescent beneath the ceiling;
- The smoke is treated as ideal gas. In particular, the smoke density varies with temperature according to the ideal gas law;
- The interactions between water droplets and smoke particles consist of a drag force only ;
- The temperature is uniform in each zone. This is a reasonable assumption when, after discharging water droplets, well-mixed steady state conditions occur in each region. This is discussed below (Figure 3). The major simplification at the moment lies in the fact that the three temperatures are prescribed, not calculated by means of heat transfer modeling. This extension, while relevant and valuable, is considered beyond the scope of the present paper. (Note that detailed heat transfer calculation would also imply a local temperature gradient, but this is not an essential feature to capture the first order effects of the water on the smoke, as discussed below);
- The shape of Zone III, i.e. the spray envelope, is calculated from individual droplet trajectories (see below);

- Water droplets are spherical and their radius does not change.
- Droplets disruption or coalescence is ignored. This is a reasonable assumption: no evidence of droplet-interaction was reported in experiments (e.g. [23]).
- All water droplets have identical diameters and discharge velocities. As such, the spray is a hollow cone and the total drag force acts on the spray envelope only. Primarily, therefore, smoke is dragged downward in the model near the spray envelope. As sketched in Fig. 3 (top figure), smoke will try to flow upward (since it is hotter than the surrounding aire) inside and outside the spray envelope, thus filling a volume inside the spray envelope. This also happens in reality when most water droplets are concentrated around the spray envelope. When most droplets are concentrated in the centre of the spray, the flow pattern becomes different (Fig. 3, bottom figure), but the end result in terms of smoke filled region inside the spray envelope remains similar as long as the central downward drag force is not too strong. For strong downward drag forces with high concentrations of water droplets in the centre of the spray, a triangular smoke shape is observed [3]. This point is reconsidered below in section 3.1.

Before developing the model, some comments are provided about the simplification in the model with respect to the flow field. Figure 3 shows a schematic sketch of possible smoke flow when droplets in the spray in reality are mainly concentrated around the manifold of the spray envelope (top figure) or more in the centre (bottom figure). The smoke flow is not explicitly taken into account in the model, but it is clear that the displacement will make the temperature inside region III more uniform, which serves as

support for this assumption made above. Smoke outside of the spray envelope is not considered in the buoyancy term below. This point is discussed below again where relevant.

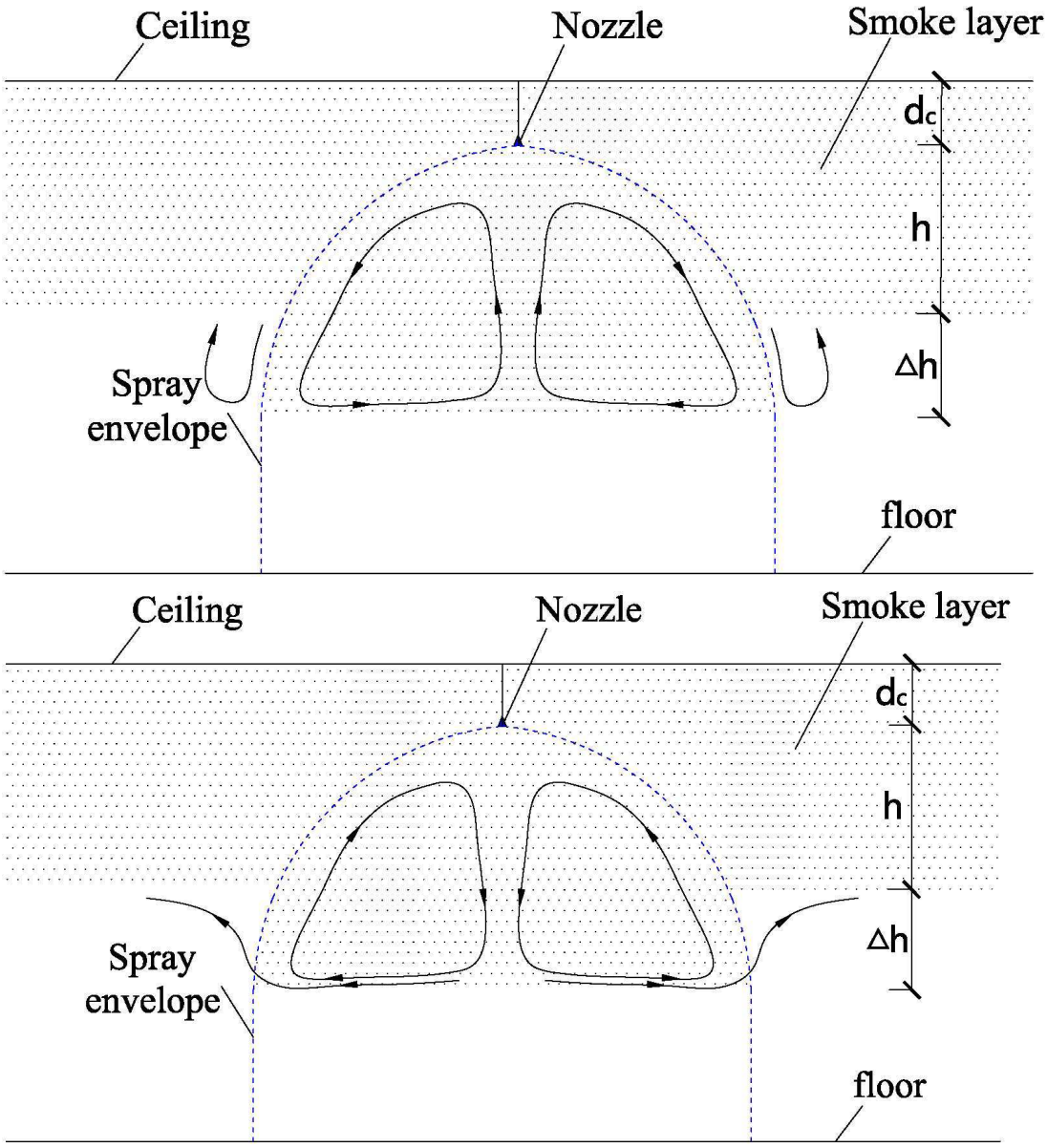

Figure 3. Schematic representation of smoke movement when droplets are mainly concentrated around the spray envelope (top) or mainly concentrated in the centre (bottom).

2.3 Individual water droplet dynamic equations

The equations for the dynamics of a single water droplet are presented. The end result will determine the volume of Zone III and the total drag force.

The spray is assumed to be axisymmetric, and the equations are written in two-dimensional form. It is straightforward to extend the model for non-axisymmetric configurations, but since this is not relevant for the sake of the present paper, we prefer to describe the equations for this simplified configuration. The z-direction is vertical and r refers to the radial direction, as shown in Figure 2. The single water droplet momentum equations then read:

$$\begin{cases} \dfrac{d(mv_z)}{dt} = mg - F_{D\_Z} \\ \dfrac{d(mv_r)}{dt} = -F_{D\_r} \end{cases} \tag{2}$$

where m is the case of a single water droplet mass, related to its diameter through:

$$m = \frac{\pi \rho_d d_m^{\,3}}{6} \tag{3}$$

The components v_z and v_r are the vertical and radial component of the droplet velocity v.

$$v = \sqrt{v_z^{\,2} + v_r^{\,2}} \tag{4}$$

The drag force F_D is modeled as:

$$F_D = C_D \frac{1}{2} \rho_i v^2 \frac{1}{4} \pi d_m^{\,2} \tag{5}$$

where $\rho_i = \rho_{i,s}$ or $\rho_{i,a}$. Since the smoke is assumed not to move in our present model formulation, the droplet velocity itself is the relative velocity, required to evaluate the drag force. The following equations are used to calculate the drag coefficient C_D [5,8,16,22]:

$$C_D = \begin{cases} 24/\mathrm{Re} & 0 \le \mathrm{Re} \le 1 \\ 12.6/\mathrm{Re}^{0.5} & 1 \le \mathrm{Re} \le 800 \\ 0.44 & 800 \le \mathrm{Re} \end{cases} \tag{6}$$

where $\mathrm{Re} = v d_m / \upsilon$ with [8]:

$$\upsilon = 1.49\times10^{-5}\times0.518\frac{T_i}{293}\left(\frac{T_i}{293}+1.55\right)^{0.7} \tag{7}$$

with $T_i = T_{i,s}$ or $T_i = T_{i,a}$ (expressed in K).

F_{D_z} and F_{D_r} read:

$$\begin{cases} F_{D\_z} = F_D \dfrac{v_z}{\sqrt{{v_z}^2 + {v_r}^2}} \\ F_{D\_r} = F_D \dfrac{v_r}{\sqrt{{v_z}^2 + {v_r}^2}} \end{cases} \tag{8}$$

According to the above equations, Eq. (2) can be rewritten as:

$$\begin{cases} \dfrac{d(v_z)}{dt} = g - \dfrac{3}{4}\dfrac{C_D \rho_i \sqrt{{v_z}^2 + {v_r}^2}\, v_z}{\rho_d d_m} \\ \dfrac{d(v_r)}{dt} = g - \dfrac{3}{4}\dfrac{C_D \rho_i \sqrt{{v_z}^2 + {v_r}^2}\, v_r}{\rho_d d_m} \end{cases} \tag{9}$$

In addition, the water droplet coordinates at each time t can be calculated from:

$$\begin{cases} \dfrac{dz}{dt} = v_z \\ \dfrac{dr}{dt} = v_r \end{cases} \tag{10}$$

Solving Eq. (9) and (10) numerically provides the individual water droplet trajectories. Some examples are presented below.

2.4 Global force analysis on the smoke layer

After discharge of the water droplets, the interface between the smoke layer and the air descends within the water spray envelope to a certain height. It is then assumed to maintain at that height. This has been observed in many experiments [2, 3, 6, 10]. The smoke stays at a certain height, determined by a balance of the downward forces acting on the smoke and the upward force. As mentioned in previous sections, the downward forces stem from the

cooling effect (net downward buoyancy in the smoke region) and the drag force from the water droplets. The upward force is the buoyancy force on the downward moved smoke by the surrounding air (which is at ambient temperature). This balance is now quantified in model equations. It results in an expression for the depth of the downward smoke displacement, Δh.

Expressing conservation of total momentum for Zone III in Figure 2 reads:

$$\dot{m}_w(v_{z,in} - v_{z,out}) + m_w g + (\rho_{i,s} - \rho_s)V_{i,s} g = (\rho_a - \rho_{i,a})V_{i,a} g \tag{11}$$

where $\dot{m}_w$ is water mass flow rate (depending on the operating water pressure and the nozzle type), and m_w is the total mass of water droplets in Zone III. This total mass is computed as $m_w = \dot{m}_w \Delta t$, with Δt the time needed for the droplets to travel through Zone III. $V_{i,s}$ and $V_{i,a}$ are determined from the water droplet trajectories:

$$\begin{cases} V_{i,s} = \int_0^h \pi r^2 dh \\ V_{i,a} = \int_h^{h+\Delta h} \pi r^2 dh \end{cases} \tag{12}$$

where h and Δh are shown in Figure2.

The first two terms on the left hand side of Eq. (11) represent the total drag force acting on smoke layer. Indeed, if the water droplets do not experience drag from the smoke, their momentum increases by gravity. If the water droplets have an initial vertical velocity $v_{z,in}$, the total momentum of the water droplets increases as: $\dot{m}_w v_{z,out} = \dot{m}_w v_{z,in} + m_w g$. If there is a total drag force F_D on the droplets, the increase in momentum is reduced: $\dot{m}_w v_{z,out} = \dot{m}_w v_{z,in} + m_w g - F_D$. Therefore, by the action-reaction principle, the total drag force on the smoke by the water droplets reads:

$$F_D = \dot{m}_w(v_{z,in} - v_{z,out}) + m_w g \tag{13}$$

The third term represents a downward buoyancy force on $V_{i,s}$ due to the cooling effect within the spray envelope. The right hand side of Eq. (11) represents the upward buoyancy force in the ambient air region.

$v_{z,in}$ can be calculated as:

$$v_{z,in} = v_{in}\cos(\theta/2) \tag{14}$$

where θ is the water spray angle and thus $\theta/2$ is the angle of injection (relative to the vertical direction). v_{in} is the orifice velocity, and read as:

$$v_{in} = \frac{4\dot{m}_w}{\pi d_n^{\,2}} \tag{15}$$

$v_{z,out}$ is determined from Eq.(9)-(10). Thus F_D (Eq. (13)) can be computed.

Consequently, Δh can be determined: In Eq. (16), F_D is computed from Eq. (13), the evolution of spray radius with height is calculated from the droplet trajectories (Eq. (9) and (10)) and the other quantities ($\rho_{i,s}, \rho_s, \rho_a, \rho_{i,a}$ and h) are input variables. Note that in Eq.(13), also $\dot{m}_w$ and $v_{z,in}$ are input variables, while m_w and $v_{z,out}$ are computed.

$$F_D + (\rho_{i,s} - \rho_s)g\int_0^h \pi r^2 dh = (\rho_a - \rho_{i,a})g\int_h^{h+\Delta h} \pi r^2 dh \tag{16}$$

If Δh as calculated from Eq. (16) is less than the distance between floor and the bottom of the hot smoke layer, the result means that the distance of the smoke layer falling down is Δh. Otherwise, the smoke layer totally loses its stability and falls down to the floor.

3. Results and discussion

After testing the model by comparing to experimental data from a test case, some model tests are reported, illustrating at the same time the model's possibilities and the sensitivity to certain parameters.

3.1 Comparison to experimental data

The model is now applied to the experimental set-up as described in [3]. In this set-up, smoke from a fire source is collected inside a hood, after which a water spray system is activated. The smoke layer thickness h equals 2m. A ZSTP-15 Sprinkler with 12.7mm orifice has been adopted in the experiments. The flow coefficient of the ZSTP-15 sprinkler is 80, so that the water mass flow rate $\dot{m}_w$ (kg/s) is calculated as [3]:

$$\dot{m}_w = \frac{80\rho_d\sqrt{10P}}{60\times10^3} \tag{17}$$

where P is the operating pressure of the sprinkler, expressed in MPa.

The Volume Median Diameter of the water droplets d_m reads [2,3,8]:

$$d_m = C_m d_n We^{-\frac{1}{3}} \tag{18}$$

Where C_m =2.33, d_n =12.7mm, and We is the Weber number:

$$We = \frac{\rho_d v_{in}{}^2 d_n}{\sigma_w} \tag{19}$$

where v_{in} is calculated from Eq.(15) and σ_w is water surface tension, $\sigma_w = 72.8\times10^{-3}\,Nm^{-1}$.

Considering the effect of the deflector of the sprinkler, the spray angle θ is taken as 180°. The ambient temperature T_a has been measured in the experiments and is applied in the model accordingly. In the depict of the set-up [3], four thermocouple trees were distributed in a circle of diameter 1.2m with the sprinkler at the center, and the vertical interval of the

thermocouples is 0.3m. The average temperature of the smoke inside the hood (T_{aih}) was measured from these thermocouples in the experiments. Therefore, it is difficult to determine T_s, $T_{i,s}$ and $T_{i,a}$ using only one reported value T_{aih}. Since the smoke hood space is not much larger than the volume of water spray envelope, it is reasonable to make the assumption $T_s = T_{i,s} = T_{i,a} = T_{aih}$ as long as Δh is not too large. Otherwise, the discrepancy among T_s , $T_{i,s}$ and $T_{i,a}$ cannot be ignored. A sensitivity study is provided below (Table 2). Note that there is only negative buoyancy if $T_{i,s} < T_s$. If $T_{i,s}$ is assumed equal to T_s, only the total drag force causes downward smoke movement.

Table 1 reveals very good agreement model results with measurements for most experiments. The trends are clearly well captured. Accuracy is in general better than with the model of [3], which relied upon the Bullen theory. In particular, $\Delta h = 0$ is never predicted, in line with the experimental observation.

For the experiments with large Δh (> 1m), agreement with the basic model is less satisfactory. A general under-prediction is observed. One reason might be that, for the cases of large Δh, a triangular shape of smoke volume is reported in [3] for cases with high concentration of water droplets in the centre of the spray. In the simplified model at hand, this is not taken into account: the bottom 'surface' of the smoke volume inside the spray is assumed to be flat (Fig. 2). As such, the upward buoyancy force for a given value Δh is higher in the model than in reality, since the volume for a certain value Δh is smaller in reality (triangular or conical shape) than in the model (essentially cylindrical shape). However, as explained below, also more cooling is to be expected for larger Δh in reality, so that a (stronger) temperature decrease inside the spray envelope must be imposed. In doing so,

the upward buoyancy term reduces (and the negative buoyancy term increases) and Δh increases. Therefore, a small sensitivity study is presented in Table 2. Accordingly, for temperature variations of only 1K affect the results vary so strongly that the experimental data are covered within the range of calculated Δh values with the present model. This mainly indicates that some experiments in [3] refer to very sensitive cases.

Sprinkler operating pressure(MPa) [3]	Water flow rate $\dot{m}_w$ (kg/s) (Calc.)	Initial water droplet velocity v_{in} (m/s) (Calc.)	Volume median diameter d_m (mm) (Calc.)	Test NO. [3]	T_a (K) [3]	T_{aih} (K) [3]	Depth of downward displacement smoke layer Δh (m)		
							Experiment [3]	Model results of [3]	Current Model ($T_s = T_{i,s} = T_{i,a} = T_{aih}$)
0.03	0.73	5.8	1.65	A1	296	309.1	**0.1**	0	**0.2**
				C1	298	329	**0.1**	0	**0.08**
0.04	0.84	6.7	1.50	A2	300	308.8	**0.4**	0.07	**0.36**
				B2	300	309	**0.3**	0.05	**0.35**
0.05	0.94	7.4	1.39	A3	296	302.5	**0.7**	0.43	**0.57**
				B3	296	303.2	**0.5**	0.32	**0.51**
				C2	298	321.8	**0.1**	0	**0.13**
0.06	1.03	8.2	1.31	A4	300	305.8	**1.1**	0.99	**Table 2**
				B4	300	306.5	**0.9**	0.76	**0.67**
0.07	1.12	8.8	1.24	A5	296	301.3	**1.8**	1.61	**Table 2**
				B5	296	302.3	**1.5**	1.15	**Table 2**
				C3	298	313	**0.3**	0.12	**0.29**
0.08	1.19	9.4	1.19	C4	298	311.9	**0.5**	0.26	**0.34**
0.09	1.26	10.0	1.14	B6	296	301.9	**2**	2.11	**Table 2**
				C5	298	311	**0.8**	0.45	**0.4**

Table 1. Summary of the tests (h=2m). 'Calc.' means that the value has been calculated. Values in bold refer to experimental data and results with the present model. Results reported in [3] with their model are presented for comparison reasons.

Test NO. [3]	T_a (K) [3]	T_{aih} (K) [3]	Depth of downward displacement smoke layer Δh (m)				
			Experiment [3]	Model results of [3]	Current Model		
					($T_{i,a} = T_{i,s} = T_s = T_{aih}$)	($T_{i,a} = T_{i,s} = T_s -1 = T_{aih}-1$)	($T_{i,a} = T_{i,s} -1 = T_s -2 = T_{aih}-2$)
A4	300	305.8	1.1	0.99	0.77	1.28	1.75
B4	300	306.5	0.9	0.76	0.67	1.08	1.4
A5	296	301.3	1.8	1.61	0.98	1.67	2.5
B5	296	302.3	1.5	1.15	0.78	1.26	1.67
B6	296	301.9	2	2.11	1.1	1.8	2.5

Table 2. Summary of the tests with Δh >1m.

3.2 Water droplets trajectories and drag force

As mentioned above, one downward force acting on the smoke is the total drag force by the droplets. This force depends on the inlet conditions for the water and the water droplet trajectories. These trajectories are followed in the model as developed. The total drag force can be computed either as a summation of the local drag forces on all individual droplets as they travel through the smoke layer, or as a result of the global balance, Eq. (13). Consistency between these two approaches has been verified in the model implementation (not shown).

Droplets trajectories are shown first for displacement through quiescent air. Isothermal conditions are assumed, at T_a = 293 K. The absolute values are presented for a nozzle diameter d_n = 10mm, but the trends are obviously much more important than the absolute values.

Figure 4 (top) shows the evolution of the vertical velocity component (left) and the total velocity (right) with vertical distance from the nozzle for a fixed water mass flow rate (1 kg/s) and water droplet diameter (1mm), for various spray angles θ. Recall that θ/2 refers to the

angle with respect to the vertical direction, i.e. $\theta = 0^\circ$ means vertical water injection, whereas $\theta = 180^\circ$ means horizontal injection. For the sake of simplicity, no change in nozzle exit area is accounted for, i.e. the inlet velocity is calculated as in Eq. (15). For obvious reasons, sufficiently far from the ceiling, all velocities evolve towards the same equilibrium value. Indeed, the droplet displacement becomes vertical (see bottom left figure of Figure 4), with a downward velocity that is essentially determined by the balance between gravity and the drag force on the droplet, the latter being determined by the droplet diameter (which is identical in all cases here). For large enough θ, the vertical velocity component never exceeds the equilibrium velocity.

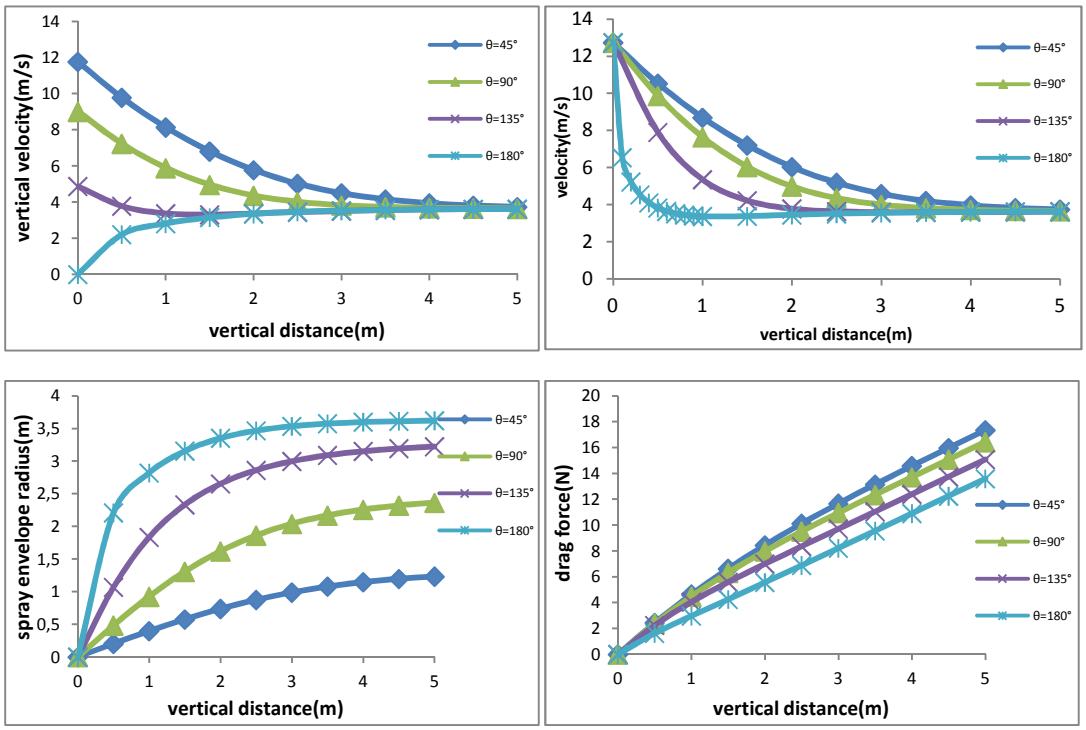

Figure 4. Evolution with vertical distance from the ceiling of the vertical velocity component (top left), velocity (top right), spray envelope radius (bottom left) and total drag force (bottom right) for fixed water mass flow rate (1 kg/s) and water droplet diameter (1mm). The lines refer to the spray angle θ at the nozzle.

This goes hand in hand with a lower drag force for higher spray angles. The bottom right figure of Figure 4 indeed illustrates a linear increase of the total drag force on the smoke with distance from the ceiling, essentially because more and more droplets exert the same drag force on the smoke, corresponding to the same equilibrium velocity in their downward displacement(parallel lines for large enough vertical distance). The difference lies in the region close to the ceiling: for smaller spray angles, the vertical velocity component is larger and the local drag force on the smoke is stronger. This effect is more pronounced for larger water mass flow rates (see below, Figure 5).

The bottom left figure of Figure 4 shows that the spray envelope radius becomes larger for higher spray angle values, for obvious reasons: the droplets are released more and more in the radial direction as θ increases.Figure 5 shows, for θ = 180°, the impact of the water mass flow rate on the droplet trajectories (left) and the total drag force (right) as function of the distance from the ceiling. As the inlet velocity increases with water mass flow rate (fixed nozzle dimension), the spray envelope radius increases accordingly. The increase in envelope radius is not linear with the water mass flow rate (or v_{in}), because the drag force increases with the square of the relative velocity. The vertical position where the displacement becomes essentially vertical is hardly affected by the water mass flow rate.

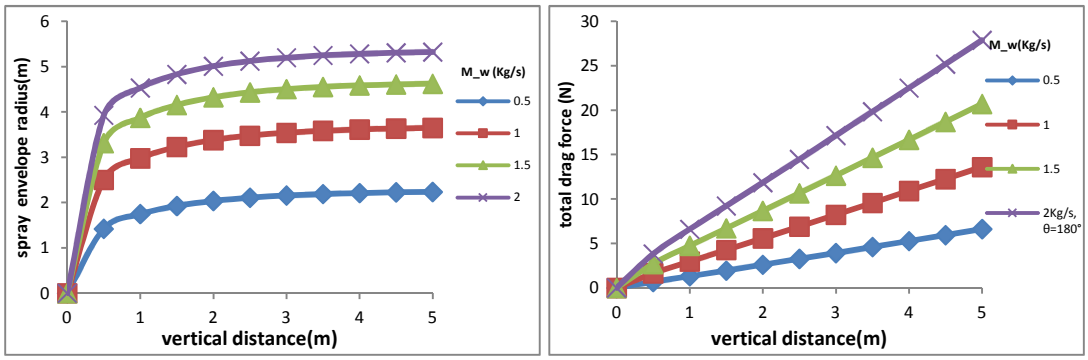

Figure 5. Evolution with vertical distance from the ceiling of the spray envelope radius (left) and total drag force (right) for fixed spray angle θ = 180^{o} and water droplet diameter (1mm). The lines refer to the water mass flow rate.

The total drag force does increase practically linearly with the water mass flow rate: the drag force per droplet is identical for all water mass flow rates in the equilibrium vertical displacement region, so that the total drag force on the smoke linearly increases with the number of droplets, which increases linearly with the water mass flow rate. The small differences near the ceiling have little influence on the total drag force. Obviously, the spray angle remains important.

Figure 6 shows, again for θ = 180^{o}, the impact of the droplet diameter on the droplet trajectories (left) and the total drag force (right) as function of the distance from the ceiling. The evolution of the spray envelope clearly shows that larger droplets result in a wider spray envelope, but also that it takes longer to reach the equilibrium vertical displacement. The total drag force becomes much higher for smaller droplets, indicating more danger for downward smoke displacement. This is as expected. Care must be taken in the interpretation of the results, though, since the water mass flow rate has been kept fixed (1kg/s), so that many more droplets are injected as the droplet diameter decreases. This explains the much higher drag force.

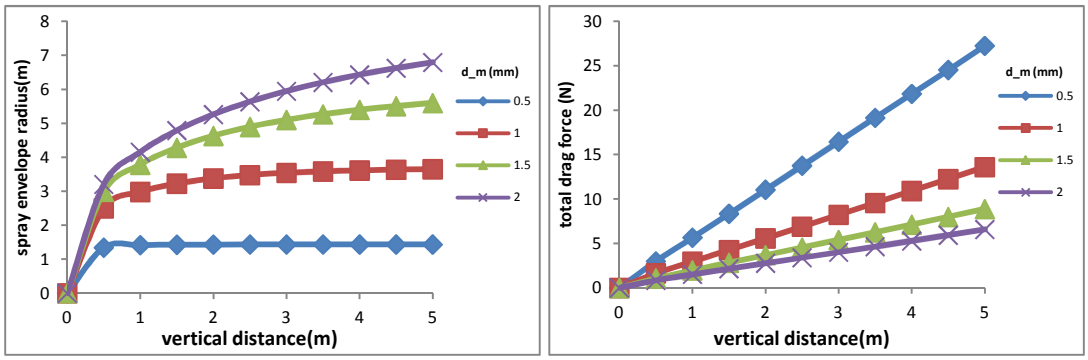

Figure 6. Evolution with vertical distance from the ceiling of the spray envelope radius (left) and total drag force (right) for fixed spray angle θ (= 180°) and water mass flow rate (1kg/s). The lines refer to the water droplet diameter (expressed in mm).

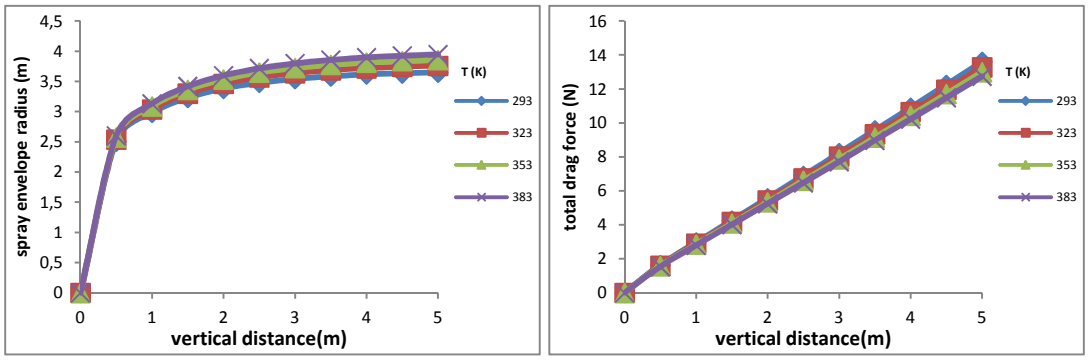

Figure 7. Evolution with vertical distance from the ceiling of the spray envelope radius (left) and total drag force (right) as function of ambient temperature for fixed spray angle θ (= 180°), water mass flow rate (1kg/s) and water droplet diameter (1mm). Lines refer to ambient temperature (in K).

Figure 7 (for spray angle 180°, water mass flow rate 1kg/s and droplet diameter 1mm) shows that the impact of the ambient temperature is negligible. There is only a small influence through Eq. (6). This implies that models for the drag force can be developed for flows at ambient temperature and be applied with confidence to flows in high temperature environment.

3.3 Prediction of downward smoke displacement

In the previous section, the evolution of the total drag force on the smoke layer has been shown to increase linearly with the distance from the ceiling, when the equilibrium vertical droplet displacement region is met. The drag force increases monotonically with the distance from the ceiling, i.e. it becomes larger for an initially thicker smoke region. This

downward drag needs to be overcome by the upward buoyancy and the position where a balance is found determines the downward smoke displacement distance Δh, (Eq.(16)).

There can, however, also be a cooling effect on the smoke:

- From the water: $T_{i,s}$ (and $T_{i,a}$) can therefore be lower than T_s. This causes a downward buoyancy force within the smoke layer: the region $V_{i,s}$ is surrounded by hotter smoke.
- From additional air entrainment in the downward (and afterwards upward, see Figure 3) smoke motion in the ambient air. As a consequence, $T_{i,a}$ can be lower than $T_{i,s}$ (and can a fortiori be lower than T_s). As a consequence, the upward buoyancy in the ambient air region becomes lower than what would be expected by using T_s in the buoyancy term.

In this section, we adopt a step-wise approach. First, no cooling effect at all is considered, i.e. $T_{i,s} = T_{i,a} = T_s$. This is the most optimistic scenario, i.e. the upward buoyancy force, necessary to counteract the downward drag, cannot be higher, so that the calculated downward smoke displacement distance Δh is minimal (for a given total drag force).

As second step, a cooling effect of the water is included, i.e. $T_{i,s} = T_{i,a} < T_s$. Then there is downward buoyancy in the smoke layer and less upward buoyancy in the air (than when T_s would be used).

Finally, additional cooling due to air entrainment in the downward smoke displacement is also included, i.e. $T_{i,s} < T_{i,a} < T_s$. For obvious reasons, since the upward buoyancy becomes weaker, higher values for Δh are found as more and more cooling effects are included.

In the results below, unless mentioned otherwise, ambient temperature is set to T_a=293K, the spray angle is 180^o and the water mass flow rate is 1kg/s. The nozzle diameter is set to 10mm here.

3.3.1 No cooling effect ($T_{i,s} = T_{i,a} = T_s$)

Figure 8 shows the downward smoke displacement Δh as function of the initial smoke layer thickness h for different smoke temperatures for droplet diameter 1mm (left) and 2mm (right). As illustrated in Figure 4, the total drag force increases linearly with the distance from the ceiling. This is to be translated here as a linear increase with initial smoke layer (provided the initial smoke layer thickness is such that the droplets reach their vertical equilibrium displacement before they leave the smoke layer; otherwise the increase is not linear, but this is of secondary importance in the discussion at hand). Consequently, the upward buoyancy force needs to be higher as well to balance the downward drag force. For a fixed temperature (or density) difference between smoke and air, this implies an increase in volume. If the spray envelope radius does not change, which is the case when the initial smoke layer thickness is such that the droplets reach their vertical equilibrium displacement before they leave the smoke layer, this implies a linear increase of Δh with h. This is confirmed in Figure 8, for large enough h.

The right panel of Figure 8 reveals that Δh is much smaller for droplets of 2mm diameter than for droplets of 1mm diameter, all the other settings (including the water mass flow rate) being identical. Figure 6 (right) revealed that the drag force is smaller, but, much more importantly, the left panel of Figure 6 shows that the spray envelope radius is much larger. As such, the volume on which the upward buoyancy force acts, is much larger (for fixed Δh).

Indeed, this increases approximately with the square of the envelope radius. Therefore, a much lower value of Δh is required to balance the (somewhat lower) total drag force.

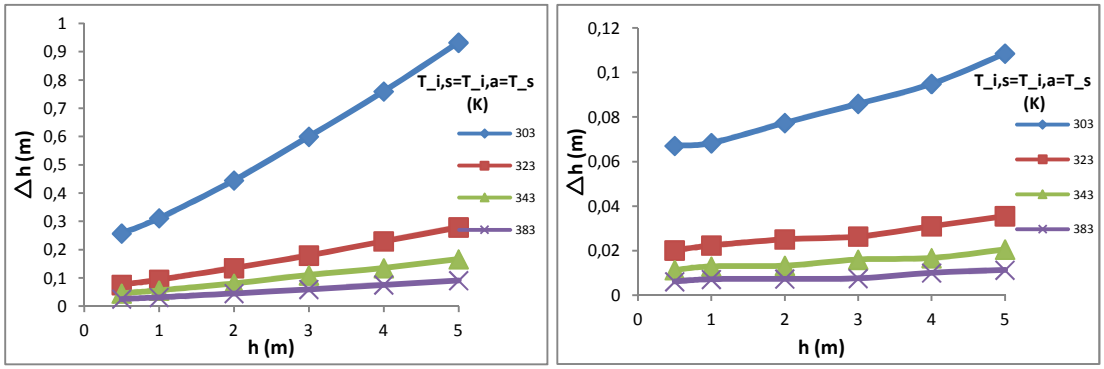

Figure 8. Downward smoke displacement distance Δh as function of the initial smoke layer thickness h for water droplet diameter 1mm (left) and 2mm (right). The lines refer to different smoke temperatures. No cooling effect ($T_{i,s} = T_{i,a} = T_s$). T_a = 293K, θ = 180° and water mass flow rate is 1kg/s.

It is noteworthy that, for initially thin smoke layers and large temperature differences between smoke and air, the downward smoke displacement distance become very small, but never zero. This is logical: there must be some downward displacement to 'activate' the upward buoyancy force. This is in contradiction with the classical Bullen theory. On the other hand, since the displacement is small under such circumstances, the Bullen theory is a good approximation of reality then.

Figure 9 reveals the effect of the water spray angle, by comparing the results with θ = 45° to θ = 180° (for droplet diameter of 1mm only). Figure 4 revealed there is some increase of the downward drag force with reduced spray angle, but the much more important effect is the reduction in spray envelope radius (also shown in Figure 4). As a result, for fixed temperature difference, a much larger downward displacement Δh is required to have the

same volume for upward buoyancy force. However, it is even worse: as Δh increases, so does the total downward drag force (see Figure 4 again). Consequently, a larger downward (drag) force needs to be overcome by the upward buoyancy, hence further increasing Δh. This explains the huge increase in Δh for smaller spray angles. For the lowest temperature difference, no solution can be found, i.e. the balance (Eq.(16)) cannot be obtained. This implies downward smoke displacement to the floor. It must be acknowledged that, in reality, the smoke is not really trapped within the spray envelope, as indicated in Figure 4. Yet, Figure 9 clearly reveals the importance of large enough nozzle spray angles to avoid strong downward smoke displacement: for smaller spray angles much more downward smoke displacement is to be expected in any case.

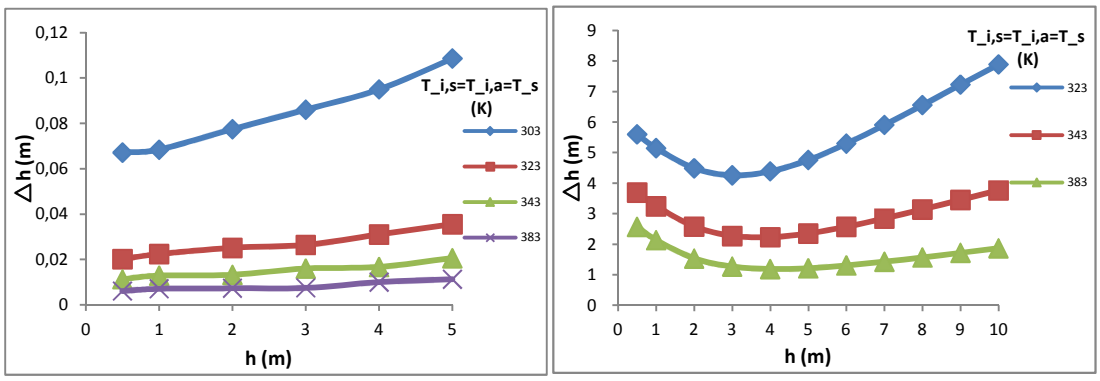

Figure 9. Downward smoke displacement distance Δh as function of the initial smoke layer thickness h for θ = 180° (left) and θ = 45° (right). The lines refer to different smoke temperatures. No cooling effect ($T_{i,s} = T_{i,a} = T_s$). T_a = 293K, water mass flow rate is 1kg/s and water droplet diameter 1mm.

The right panel of Figure 9 also shows an artifact with the smaller spray angle, namely that Δh does not vary with h in a monotonic manner (in contrast to what is observed for θ = 180°). The reason is that, for small values of h, the spray envelope radius is still very small at the

bottom of the smoke layer (Figure 4). Consequently, larger values for Δh are required to have a sufficiently large volume in which the upward buoyancy force counteracts the downward drag force. For large enough h, the spray envelope radius does not change anymore with h and the linear increase of Δh with h is recovered (in line with the linear increase of the total drag force).

Note that during the initial stage of a developing fire (h not get large) this result indicates that Δh is larger for smaller smoke thicknesses for small spray angle, while the opposite is true for large spray angles. This clearly reveals the importance of the spray angle.

3.3.2 Cooling effect by water ($T_{i,s} = T_{i,a} < T_s$)

Figure 10 presents the same results as Figure 8, but with introduction of a cooling effect by the water. In all cases, the choice $T_{i,s} = T_s - 5K$ is made here. No additional cooling in the air region is accounted for ($T_{i,a} = T_{i,s}$). As explained above, the cooling effect triggers downward buoyancy in the smoke region and less upward buoyancy in the air region. Not surprisingly, higher values for Δh are found in Figure 10 than in Figure 8. As explained in the previous section, the effect of larger Δh additionally leads to higher downward drag forces to be balanced, so the effect is stronger than what would be expected from the loss in buoyancy alone. For the sake of clarity, a zoom is presented of the results for the 1mm droplets and the left hand side of Figure 8 is repeated as bottom right figure in Figure 10, in order to facilitate the comparison. Clearly, the effect of 5K smoke temperature reduction by the water results in a strong increase in Δh. Note that the value of Δh becomes extremely sensitive to the cooling effect in the smoke when the temperature difference between

smoke and air ($T_s - T_a$) is small. The results for $T_s - T_a$ = 10K are not even on the graph in the bottom left figure.

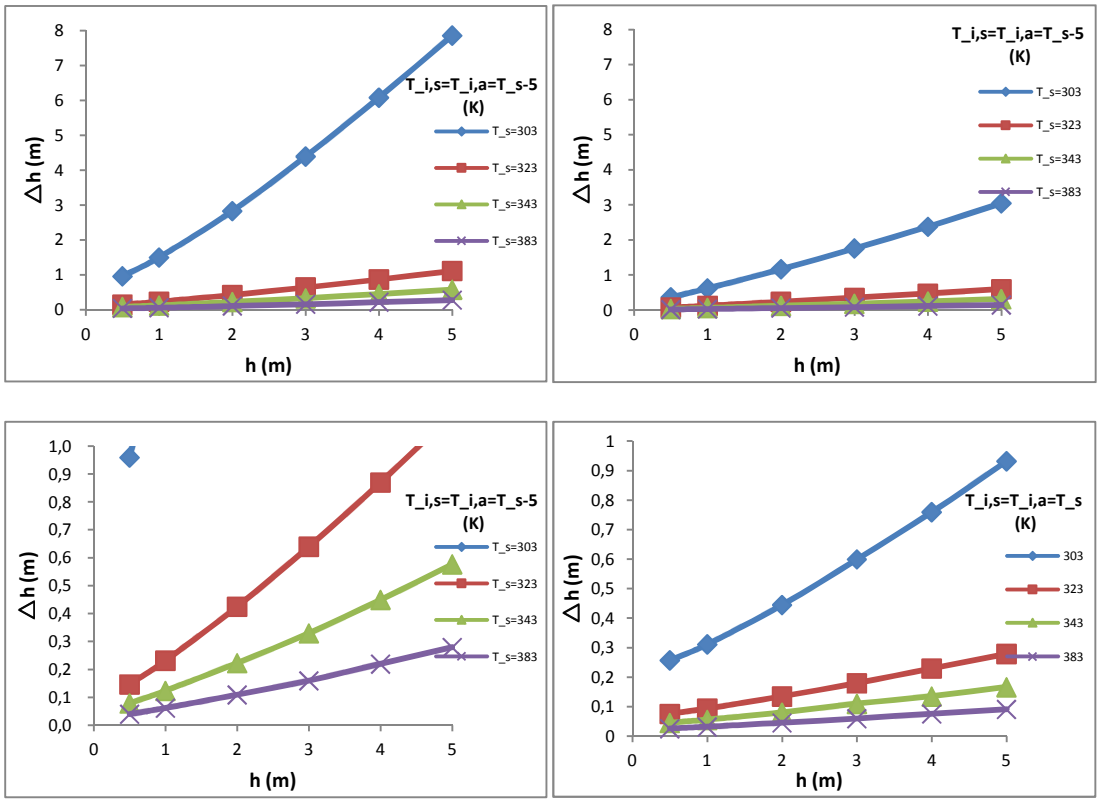

Figure 10. Downward smoke displacement distance Δh as function of the initial smoke layer thickness h for water droplet diameter 1mm (top left) and 2mm (top right). The lines refer to different smoke temperatures. Water cooling effect ($T_{i,s} = T_{i,a} = T_s$-5). T_a = 293K, θ = 180° and water mass flow rate is 1kg/s. Bottom left: zoom of top left figure; bottom right: copy of left panel of Figure 8, to be compared to bottom left figure.

3.3.3 Cooling effect by water and air ($T_{i,s} < T_{i,a} < T_s$)

Figure 11 presents the same results as Figures 8 and 10, but with introduction of not only a cooling effect by the water, but also additional cooling by air entrainment into the smoke logging region. This additional cooling due to air entrainment can lead to (much) stronger downward smoke layer displacement, as explained next. In all cases, the choice $T_{i,a} = T_{i,s} - 5K = T_s - 10K$ is made here. As a consequence, no results are shown for the case $T_s - T_a = 10K$, as there is no upward buoyancy in the air region (so that the smoke moves downward to the floor). The choice for temperature differences of 5 K is arbitrary. It only serves to illustrate trends in the results.

As explained above, the cooling effect triggers downward buoyancy in the smoke region and less upward buoyancy in the air region. Not surprisingly, higher values for Δh are found in Figure 11 than in Figure 9 or Figure 10, since the upward buoyancy is now further reduced by the lower value for $T_{i,a}$. For high enough temperature difference between smoke and air (large $T_s - T_a$), the results remain relatively unaffected. For smaller temperature differences, the effect is much more pronounced (e.g. a 30% increase in Δh for $T_s - T_a = 30K$ ($T_s = 323K$) for $T_{i,a} = T_{i,s} - 5K$ as compared to $T_{i,a} = T_{i,s}$). As explained in the previous section, the effect of larger Δh additionally leads to higher downward drag forces to be balanced, so the effect is stronger than what would be expected from the loss in buoyancy alone.

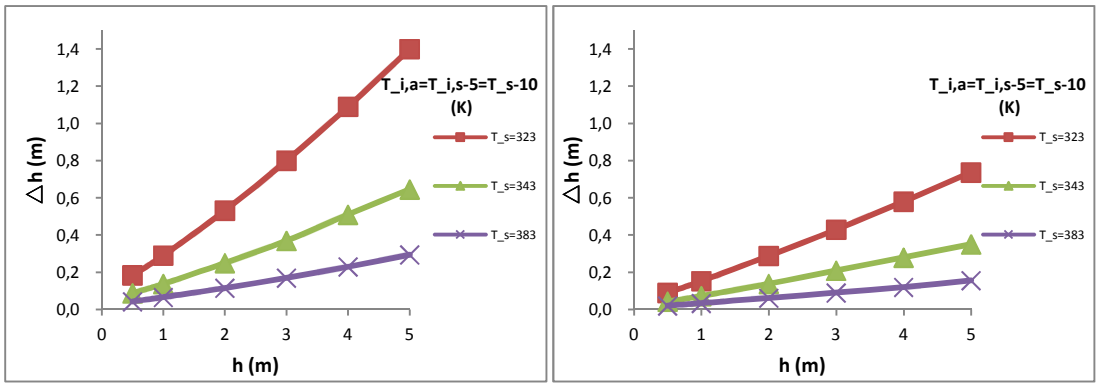

Figure 11. Downward smoke displacement distance Δh as function of the initial smoke layer thickness h for water droplet diameter 1mm (left) and 2mm (right). The lines refer to different smoke temperatures. Water and air cooling effect ($T_{i,a} = T_{i,s} - 5K = T_s - 10K$). T_a = 293K, $\theta = 180^o$ and water mass flow rate is 1kg/s.

4. Limitations of the model

Since the analytical model is simple, it is important to recall its limitations in order to avoid improper use.

The model as presented is simplified in the sense that no fluid dynamics equations are solved for the gas phase. As such, care must be taken when applying the model in more complex situations, e.g. in regions where the smoke is moving. Such displacement can be horizontal (e.g. a smoke layer in a tunnel configuration) or vertical (e.g. in the buoyant region above the fire source), or a combined displacement (e.g. in the ceiling jet turning region). Horizontal displacement can be incorporated relatively easily, since the main phenomena – downward drag and buoyancy – occur in the vertical direction, i.e. perpendicular to the smoke displacement. The main alteration to the model would be the relative velocity in the drag force and the fact that the droplet trajectories will no longer be axisymmetric. Vertical gas phase displacement is more complex, as the upward buoyant flow would also affect the downward falling droplets and may indeed make them move upward if the downward droplet momentum is not sufficient to overcome the upward momentum in the gas phase. Such an effect is not yet incorporated in the model. However, if this is the case, there is also no issue of downward smoke displacement due to the water spray.

No heat transfer model has been incorporated at present. This will be done in future work. This is relevant mainly for low smoke temperatures since, as illustrated, the downward smoke displacement becomes strongly dependent on small temperature variations under such circumstances.

5. Conclusions

In the paper at hand, an analytical model for the effect of a water spray on a fire-induced smoke layer has been developed from first principles. The simplifications introduced have been highlighted. It has been illustrated that the classical Bullen theory needs to be revised. The balance is essentially indeed between downward drag and upward buoyancy, as in the Bullen theory, but there is also net downward buoyancy in the cooled region in the smoke layer. More importantly, in contrast to what is generally assumed in existing models, the upward buoyant force only applies to the region where the smoke is surrounded by ambient air, not to the entire spray envelope. An important consequence is that there is always some smoke descent and the Bullen criterion to determine whether a smoke layer is stable or not, does not apply. Only under the circumstances of an initially thin smoke layer, the Bullen theory provides a good approximation to reality.

From an extensive sensitivity study, varying the water spray angle at the nozzle, the water droplet diameter, the smoke layer temperature, and inclusion or not of the cooling effect by water and air entrainment in the downward smoke displacement, the following trends have been explained for all cases studied:

- The downward smoke displacement is more pronounced for smaller droplets (for fixed water mass flow rate), mainly because the water spray envelope equilibrium radius is smaller. The upward buoyancy force then requires a larger smoke descent to have sufficient volume. As the downward drag force increases with smoke descent, the effect is stronger than what is expected from the decrease in upward buoyancy force (due to the reduction in volume) alone.

- The downward smoke displacement is more pronounced for lower smoke layer temperatures, due to a reduced upward buoyancy force (smaller temperature or density difference). Since the downward drag force increases with smoke descent, the effect is again stronger than what is expected from the decrease in upward buoyancy force alone.

- For large enough water spray angle at the nozzle, the downward displacement increases monotonically with initial smoke layer thickness, due to a (more or less linearly) increasing downward drag force.

- A smaller water spray angle at the nozzle results in stronger downward smoke displacement. The variation of downward smoke displacement depth with initial smoke layer thickness is also non-monotonic: stronger descent of smoke for thinner smoke layer, but beyond a critical smoke layer thickness also again a stronger descent with increasing smoke layer thickness.

Finally, the accuracy of the model as presented is illustrated by means of an experimental data set [3]. A small sensitivity study has been added to illustrate that the cooling effect for stronger smoke descent can affect the results substantially, particularly for small temperature differences between smoke and air.

Acknowledgements

This research was supported by the Natural Science Foundation of China (NSFC) under Grant No. 50978206, by the lotus project and Special Research Fund – Gent University (Belgium) (BOF) under Grant No.01SF0111.

References

[1] D. Drysdale. An Introduction to Fire Dynamics. John Wiley and Sons, New York, 2nd edition, 2002.

[2] M. L. Bullen. The Effect of a Sprinkler on the Stability of a Sprinkler on the Stability of a Smoke Layer beneath a Ceiling. Fire Research Note 1016, Fire Research Station, Borehamwood, UK, 1974, 1-11.

[3] K. Y. Li, L. H. Hu, R. Huo, Y.Z. Li, Z.B. Chen, S.C. Li and X.Q. Sun, A Mathematical model on interaction of smoke layer with sprinkler spray. Fire Safety Journal, 44 (2009), 96-105

[4] K. Y. Li, J. Spearpoint. Simplified Calculation Method for Determining Smoke Downdrag Due to a Sprinkler Spray. Fire Technology, 47(2001), 781-800

[5] L. Y. Cooper. The Interaction of an Isolated Sprinkler Spray and a Two-Layer compartment Fire Environment. Int. J. Heat Mass Transfer, Vol.38, No.4(1995), 679-690

[6] C. F. Zhang. Study on the Dynamics of Smoke Movement under Some Typical Sprinklers. PhD Thesis, University of Science and Technology of China, Hefei, Anhui, China, 2006

[7] K. Y. Li, M. J. Spearpoint. A Review of Instability Criteria of Smoke Layers under Sprinkler Spray. International Symposium on Fire Science and Fire Protection Engineering, Hefei, China, 17 Oct 2009, 70-77.

[8] W. K. Chow, B. Yao. Numerical Modeling for Interaction of a water spray with smoke layer. Numerical Heat Transfer, Part A, 39(2001), 267-283.

[9] A. J. GARDINER. The Mathematical Modelling of the Interaction between Sprinkler Sprays and the Thermally Buoyant Layers of Gases from Fires. PhD thesis, South Bank

University, 1988.

[10] C. Williams. The Downward Movement of Smoke due to a Sprinkler Spray. PhD thesis, South Bank University, 1993.

[11] Dong Yang, Ran Huo, etc.. A Fire Zone Model Including the Cooling Effect of Sprinkler Spray on Smoke Layer. Fire Safety Science-Proceedings of the Ninth International Symposium, 919-930.

[12] C.F.Zhang, R. Huo, Y. Z. Li. Stability of Smoke Layer under Sprinkler Water Spray. ASME's 2005 Summer Heat Transfer Conference, San Francisco, 2005.

[13] W.K. Chow, A. C. Tang. Experimental Studies on Sprinkler Water Spray-Smoke Layer Interaction. Journal of Applied Fire Science, Vol. 4, No. 3, 171-184, 1994.

[14]Morgan HP. Heat transfer from a buoyant smoke layer beneath a ceiling to a sprinkler spray 1. A tentative theory. Fire Mater 3:27-32, 1979

[15]Morgan HP. Heat transfer from a buoyant smoke layer beneath a ceiling to a sprinkler spray. 1. An experiment. Fire Mater 3:34-38, 1979

[16] W. K. Chow, Y. L. Cheung. Simulation of sprinkler-hot layer interaction using a field model. Fire and Materials, Vol. 18, 359-379, 1994

[17]Jeremiah P. Crocker, Ali S. Rangwala, Nicholas A. Dembsey. Investigation of Sprinkler Sprays on Fire Induced Doorway Flows. Fire Technology, 46, 347-362, 2010.

[18] Y. F. Li, W. K. Chow. Study of Water Droplet Behavior in Hot Air Layer in Fire Extinguishment. Fire Technology, 44, 351-381, 2008

[19] Gerard G. Back, Craig L. Beyler, Rich Hansen. A quasi-steady-state model for predicting fire suppression in spaces protected by water mist systems. Fire Safety Journal 35(2000)

327-362

[20] G. Grant, J. Brenton, D. Drysdale. Fire suppression by water sprays. Progress in Energy and Combustion Science 26(2000) 79-130

[21] Herterich O. Water as an extinguishing agent. Heidelberg: Alfred Huthig Publishing Company, 1960.

[22] William A. Sirignano. Fluid Dynamics and Transport of Droplets and Sprays. Cambridge university press, 1999

[23] M. St-Georges, J. M. Buchlin. Detailed single spray experimental measurements and one-dimensional modeling. Int. j. Multiphase Flow Vol. 20, No. 6, pp.979-992, 1994

[24] Krishnan, G., Gakkar, R.P., Prakash, S., “Water Droplet Evaporation in Fire Plumes”, ICLASS-91 Proceedings, National Institute of Standards and Technology, Gaithersburg, MD, pp. 97-104, 1991.